33rd Annual International Conference of the IEEE EMBS
Boston, Massachusetts USA, August 30 - September 3, 2011

Analysis of Integrated Optofluidic Lab-on-a-chip Fluorescence Biosensor Based on Transmittance of Light through a Fluidic Gap

Narayan Krishnaswamy, T. Srinivas, *Senior Member, IEEE.*, and G. Mohan Rao.

***Abstract*— Sensitivity analysis is an important aspect to be looked into while designing lab-on-a-chip systems. In this paper we will be showing with appropriate design that the best sensitivity of the fluorescence biosensor is achieved for an optimal width of fluidic gap, corresponding to a particular mode spot size. We will be also showing that the sensitivity of the biosensor is affected by efficiency of light coupling, which is influenced by changes in the width of fluidic gap, refractive index of the fluid and higher order modes.**

I. Introduction

INTEGRATION of microfluidics with optical detection is one of the challenges for lab-on-a-chip based devices. Optofluidics is a new branch within photonics which attempts to unify concepts from optics and microfluidics [1]. Unification of photonics and microfluidics enable us to carry out clinical analysis of human physiological fluids through optical sensing and detection. Current optical sensors so far reported [2] have not adopted any specific design to calculate fluidic gap width. The width of the fluidic gap has an important influence on the sensitivity of the biosensor. In this paper we have arrived at a mathematical formulation to calculate optimum width of fluidic gap. Moreover in [2] the source of light and photo-detection modules are external to the sensor microchip, this invariably increases the size of the device and hence preventing their use in point of care applications. "In-built" source of light (organic light emitting diodes) which would form integral part of the lab-on-a-chip device has been fabricated and light emission from it has also been tested. The optical power output from the organic light emitting diode (OLED) has been measured and is presented in this paper. This monolithically integrated source of light would not only help in further miniaturization of lab-on-a-chip device but would also improve sensitivity of such device. Design of such lab-on-a-chip device is presented in this paper. Schematic diagram of an integrated lab-on-a-chip (LoC) device is shown in Fig. 1(a). This device would contain an on-chip light source which is an organic light emitting diode (OLED) [3], photo-detection modules (PD), microfluidic channel containing the samples to be analyzed and waveguides both for guiding the light and to collect the fluorescence signal from the analyte [4],[5]. The arrows in Fig 1(b) represent direction of travel of light in the input and output waveguides. Transmittance of light is along the plane of the paper from left to right. Dots in the fluidic channel shown in Fig 1(b) represent the direction of flow of fluid perpendicular to the plane of the paper (towards the observer). Fluidic flow and transmittance of light are in mutually perpendicular directions. Fig. 1(c) further clarifies the mutually perpendicular directions of flow of fluid and transmittance of light. The transmission of light from the source through the intervening waveguides, fluidic gap, and the emergence of the light after the light analyte interaction, and eventual detection of the output light by photodiode necessitates an efficient integrated waveguide design.

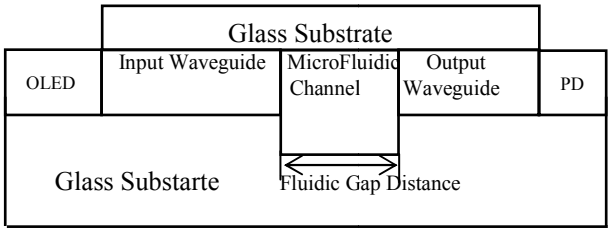

Fig. 1(a). Schematic diagram of Integrated Lab-on-a-Chip device showing the front view.

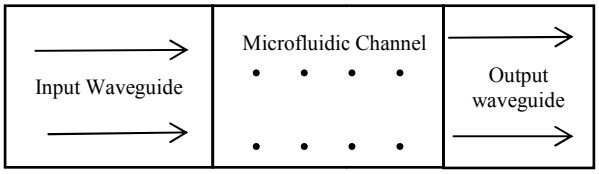

Fig. 1(b). Schematic diagram showing direction of fluid flow and light passing through it.

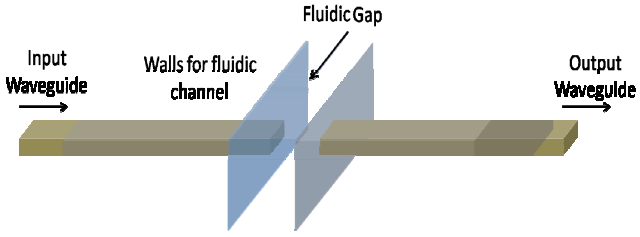

Fig. 1(c). Schematic isometric view of fluidic channel and waveguides.

Manuscript received March 28, 2011.

Narayan Krishnaswamy is a research student with department of Instrumentation and Applied Physics, Indian Institute of Science, Bangalore 560012, India (phone: 91-080-41685477; fax: 91-080-23600683; e-mail: narayank@airtelmail.in , chintu_k@vsnl.com , narayan@isu.iisc.ernet.in).

T. Srinivas is an Associate Professor with the department of Electrical and Communication Engineering, Indian Institute of Science, Bangalore 560012, India (e-mail: tsrinu@ece.iisc.ernet.in).

G. Mohan Rao is a Professor with the department of Instrumentation and Applied Physics, Indian Institute of Science, Bangalore 560012, India (e-mail: gmrao@isu.iisc.ernet.in).

II. Integrated Optical Waveguide Design

For designing integrated channel waveguide the net effective refractive index is required. The refractive index of various layers of the integrated channel waveguide is shown in Fig.2. Diffusion of ions such as Ag^+ produces refractive index changes in the order of 1% with respect that of the glass substrate [6],[7]. After silver ion diffusion another layer, which has a higher refractive index such as commercially available acrylate based polymer, can be deposited to produce light confinement in a narrow channel. In order to solve the dispersion equation for the waveguide structure, we use the effective index method where by the three dimensional channel waveguide problem is converted into a two dimensional problem. This is done by splitting the channel waveguide into two slab waveguides, one in depth and another in width direction. Mathematical solution is obtained by considering the planes of the waveguides in mutually perpendicular planes (depth wise and width wise) sequentially.

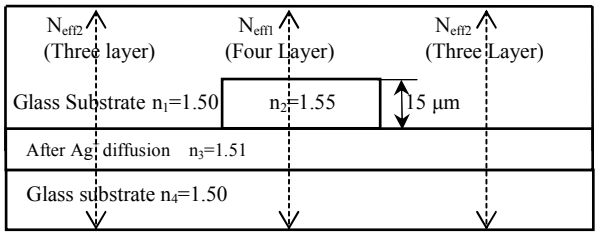

Fig. 2. Schematic front view showing different refractive indices of the loaded channel waveguide.

The dispersion equation of a four layer slab waveguide (considering firstly in depth wise direction only i.e., from top to bottom along plane of paper) is given by [8].

$$(\alpha_3+i\alpha_4)\left[(\alpha_2^2-\alpha_3\alpha_1)\tan(\alpha_2 T)-\alpha_2(\alpha_3+\alpha_1)\right]+ e^{-2\alpha_3 T}(\alpha_3-i\alpha_4)\left[(\alpha_2^2+\alpha_3\alpha_1)\tan(\alpha_2 T)+\alpha_2(\alpha_3-\alpha_1)\right]=0 \quad (1)$$

Where,

$$\alpha_1 = \sqrt{(\beta^2 - k_0^2 n_1^2)}, \alpha_2 = \sqrt{(k_0^2 n_2^2 - \beta^2)}$$

$$\alpha_3 = \sqrt{(\beta^2 - k_0^2 n_3^2)}, \alpha_4 = \sqrt{(k_0^2 n_4^2 - \beta^2)}$$

$k_0 = 2\pi/\lambda$, λ = wavelength in micrometer (μm), β = propagation constant of the four layer slab waveguide, $n_1=n_4$= refractive index of glass substrate, n_3 = refractive index of diffused region, n_2= refractive index of core region, T = thickness of the diffused and loading region in micrometer. After solving for above mentioned dispersion equation we find effective index of four layer slab waveguide $Neff_1$ which is given by

$$Neff_1=\beta/k_0 \quad (2)$$

Dispersion equation of a three layer slab waveguide [9] is well known. By solving the same in depth wise direction we find effective index N_{eff2} for a three layer slab waveguide.

$$V\sqrt{(1-b)} - 2\tan^{-1}\sqrt{\frac{b}{(1-b)}} = m\pi \quad (3)$$

Where,

$$b = \frac{(\beta_1^2 - k_0^2 n_4^2)}{k_0^2(n_3^2 - n_4^2)}, V = k_0 d\sqrt{(n_3^2 - n_4^2)}$$

$k_0 = 2\pi/\lambda$, λ = wavelength in micrometer, V = Normalized frequency, d= depth of the waveguide in micrometer (μm), m=mode number. β_1=propagation constant of the three layer slab waveguide. b= normalized propagation constant.

$$N_{eff2} = \beta_1/k_0 \quad (4)$$

The complete solution of the channel waveguide is found after finding the overall final effective refractive index by solving (5) in width wise direction (i.e., perpendicular to the plane of the paper).

$$V_{final}\sqrt{(1-b_{final})} - 2\tan^{-1}\sqrt{\frac{b_{final}}{(1-b_{final})}} = m\pi \quad (5)$$

Where

$$b_{final} = \frac{(\beta_{final}^2 - k_0^2 N_{eff\,2}^2)}{k_0^2(N_{eff\,1}^2 - N_{eff\,2}^2)}, V_{final} = k_0 w\sqrt{(N_{eff\,1}^2 - N_{eff\,2}^2)}$$

w = width of the waveguide in micrometer, β_{final} = final propagation constant of the complete channel waveguide b_{final} = final normalized propagation constant of the complete channel waveguide, V_{final} = Final normalized frequency.

Thus from the above equation various values of final normalized propagation constant can be evaluated for various waveguide widths.

Variation of normalized propagation constant with respect to different waveguide widths gives rise to dispersion curves which are shown in Fig.3. We see from Fig.3, that with reference to waveguide width of 3 micrometer (for a waveguide depth of 15 micrometer) the corresponding dispersion curve is up to third order mode, and when width is 5 micrometer then dispersion curve is up to fifth order mode.

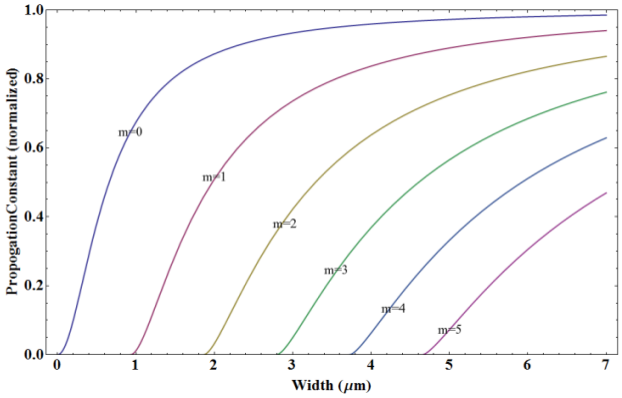

Fig. 3. Plot of Normalized propagation constant of the waveguide verses width of the waveguide for a depth of 15 micrometer for different modes.

III. Transmittance of the Light Through the Fluidic Gap

Referring to Fig. 1(a), Fig. 1(b) and Fig. 1(c) the light after being guided by the input waveguide will traverse through the fluidic gap. The light beam will spread while traversing through the fluidic gap, and thus optical mode spot size will undergo a change and will increase (due to spreading of the light). Hence the mode spot size of light

coupling with the output waveguide (near the PD) will not be the same as it was at the time of entering the gap, thus there will be a mode mismatch between the light entering the gap and the light emerging from the fluidic gap. We find out this mode mismatch and thus the amount of light coupling the output waveguide is determined. There by we can know the light coupling efficiency. Once coupling efficiency is known we can infer about the sensitivity of the sensor.

By using effective index method mathematically we have converted the three dimensional waveguide problem to a symmetrical two dimensional problem. Therefore the field profile of the input waveguide $\phi_1(x)$ and the field profile of the output waveguide $\phi_2(x)$ would be symmetrical as a function of Cosine Kx in the region, 0≤ x≤ (width of waveguide/ 2) and would decay exponentially in the region, x >(width of the waveguide/2). This is shown in Fig. 4 below.

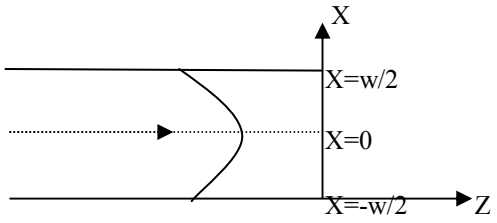

Fig. 4. Schematic diagram showing various regions of the final symmetrical waveguide.

The field of input waveguide $\phi_1(x)$ can be written as

$$\phi_1(x) = \begin{cases} B \cos KX \text{ for } 0 \le X \le (w/2). \\ Ce^{-\alpha X} \text{ for } X>(w/2) \end{cases} \quad (6)$$

$$K = \sqrt{k_0^2 N_{eff\,1}^2 - \beta_{final}^2}, \alpha = \sqrt{\beta_{final}^2 - k_0^2 N_{eff\,2}^2}$$

Where B and C are arbitrary constants, $k_0=2\pi$/wavelength, β_{final} = final propagation constant of the input loaded channel waveguide, w = width of the waveguide in micrometer, N_{eff1} and N_{eff2} are the effective indices shown in "Fig. 2" and have been taken from "(2)" and "(4)" respectively.

The output waveguide structure has a similar geometry like that of the input waveguide.

On similar lines, we can define the field of the output waveguide $\phi_2(x)$ as

$$\phi_2(x) = \begin{cases} E \cos K_2 X \text{ for } 0 \le X \le (w/2) \\ Fe^{-\alpha_2 X} \text{ for } X>(w/2) \end{cases} \quad (7)$$

$$K_2 = \sqrt{k_0^2 N_{eff\,1}^2 - \beta_{2\,final}^2}, \alpha_2 = \sqrt{\beta_{2\,final}^2 - k_0^2 N_{eff\,2}^2}$$

Where E and F are arbitrary constants, K_2 and α_2 are similar to K and α except that they are defined for output waveguide, β_{2final}= final propagation constant of the output loaded channel waveguide (near the PD) which found by using (1) to (5).

The coupling between $\phi_1(x)$ and $\phi_2(x)$ is represented by overlap integral and is given by the relation

$$\tau = \int \phi_1(x)\phi_2^*(x)dx \quad (8)$$

Where, τ = overlap integral.

The above "Equation (8)", is normalized. The normalized overlap integral τ_{nor} is given by

$$\tau_{nor} = \frac{\int_{-\infty}^{\infty} \phi_1(x)\phi_2^*(x)dx}{\sqrt{\int_{-\infty}^{\infty} \phi_1^2(x)}\sqrt{\int_{-\infty}^{\infty} \phi_2^{*2}(x)}} \quad (9)$$

If there is no gap between the waveguides then the mode mismatch will be zero and the coupling efficiency would be 100%. Now if we introduce a gap between the two waveguides, then the mode mismatch will increase, leading to drop in amount of light coupling with the output waveguide, this is caused due the fact that as the light beam propagates in the gap the mode spot size of the light coming out of the input waveguide $\phi_1(x)$ increases thus leading to mode mismatch. Using "(6)" to "(9)", a custom made program has been developed to plot the transmittance curve for various mode spot sizes.

To find the light coupling efficiency, we vary the spot size of the field emerging from the input waveguide $\phi_1(x)$ and find out light coupling with the output waveguide $\phi_2(x)$ using (9). In order to correlate variation of mode mismatch with the actual distance travelled by the light beam we use the beam propagation method described in [10],[11], by which we can correlate the distance travelled by the light for the corresponding spot size (for a particular wavelength and refractive index). Coupling efficiency can be inferred from the amount of optical power associated with the light coupling the output waveguide. Lesser is the mode mismatch greater will be the optical power and hence better coupling efficiency. Whereas greater is the mode mismatch lesser will be the optical power implying poor coupling efficiency. As the light travels through fluidic gap, optical power associated with it reduces and thus the coupling efficiency reduces with respect to the distances travelled by light (i.e., fluidic gap distances).

Fig.5 shows optical power variation as a function of gap distances (distance travelled by light in fluidic gap). Fig. 5 contains transmittance curves when spot size is of 5 micrometres and the refractive index of fluid is 1.37. It is seen from Fig. 5, that the first order mode (m_1) decays faster than the fundamental mode (m_0) and second order (m_2) decays faster than first order mode (m_1). This shows that higher order modes decay faster than lower order modes. Fig. 5 also indicates when all the modes are present, their combined effect (combined mode m_c) results in decay of light faster than fundamental mode itself (m_0). Since the distance which the light can travel is greatly influenced by the spot size and the fluidic refractive index, therefore curves similar to Fig. 5 have been plotted for different refractive indices on Fig. 6 and various spot sizes in Fig 7. The transmittance curves of Fig. 6 and Fig. 7 indicates the effect of change in refractive index and spot sizes on the rate of optical power drop as the light travels through the fluidic gap.

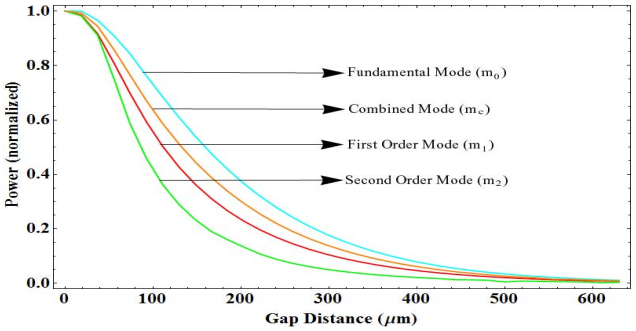

Fig. 5. Transmittance curve for various optical modes for a 5 micrometer spot size and for a refractive index of 1.37.

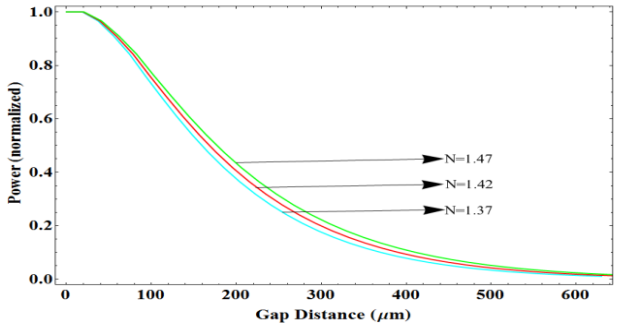

Fig. 6. Plot show the transmittance curve for a five micrometer spot size for fundamental mode and for different refractive indices of fluid.

In Fig.6, the effect of changes in refractive index N of the fluid contained in the gap is shown. As seen from the figure lower the refractive index faster is the light decay. Fig.7 shows the transmittance curve for various spot sizes from 5 micrometer to 32 micrometer. We can clearly see that smaller the spot size faster is the light decay, and larger the spot size slower is light decay. In other words if we have a smaller mode spot size then fluid gap width can be much smaller. On the other hand if we have a larger spot size then the fluidic gap width needs to be larger. The dotted curves in the Fig. 7 indicates combined effect of fundamental, first order and second order modes, thick lines in the curve indicate fundamental mode corresponding to a particular spot size.

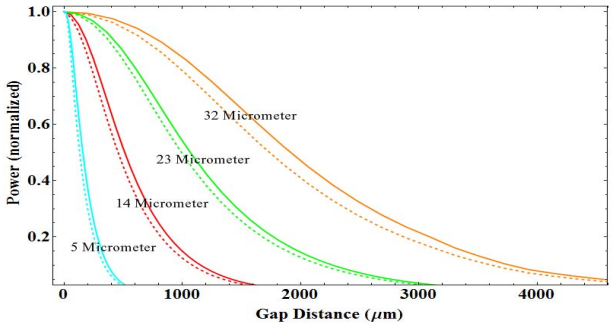

Fig. 7. Plot shows transmittance curves for different spot sizes, the dotted lines indicate combined mode, thick lines in the plot indicate fundamental mode the refractive index being 1.37.

IV. Sensitivity Analysis of the Biosensor.

In order to find out the sensitivity of the biosensor we take the slope (elemental change in power/ elemental change in refractive index of the fluid contained in the gap) of the transmittance curve. A plot of this slope verses fluidic gap distance is shown in Fig. 8. This plot is for 5 micrometer spot size and for fundamental mode as well as for combined mode (i.e., is combined effect of fundamental, first order and second order modes). We find that maximum sensitivity is achieved when the width of the gap is 100 micrometer. We also infer that the combined mode (i.e., effect of fundamental, first and second order mode) achieves better sensitivity compared to fundamental mode alone. Similarly Fig. 9 shows the plot of slope verses gap distance for spot sizes of 23 micrometer and 32 micrometer. In Table 1 ideal fluidic gap width for various spot sizes to achieve maximum sensitivity is given. From Table 1 we can see that smaller is the spot size, smaller can be the fluidic gap width. However as we increase the spot size allowable fluidic gap width also increases.

TABLE I

Sl No.	Optical Spot Size	Ideal Fluidic gap width to achieve best sensitivity
1.	5 micrometer	100 micrometer
2.	14 micrometer	250 micrometer
3.	23 micrometer	750 micrometer
4.	32 micrometer	1300 micrometer

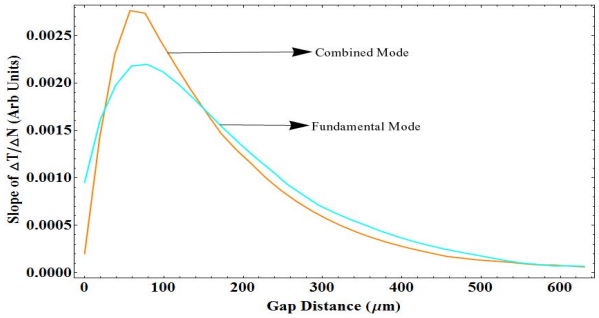

Fig. 8. Plot of slope verses gap distance for fundamental and combined mode for a mode spot size of 5 micrometer.

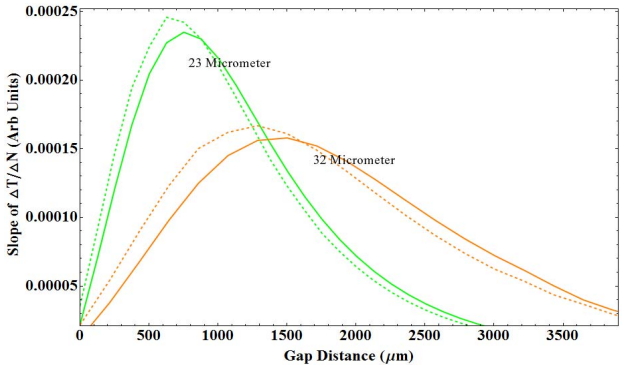

Fig. 9. Plot of slope verses gap distance for spot sizes of 23 and 32 micrometer, the dotted lines indicate combined mode, thick lines in the plot indicate fundamental mode.

V. Experimental Validation

Design data pertaining to best sensitivity for various spot sizes corresponding to different fluidic gaps is given in

Table 1. In the experiment carried out earlier [12], it has been reported that for a waveguide width of 30 microns, sensitivity vastly improved when fluidic gap distance was increased from 100 micrometer to 1000 micrometer. From Table 1 it can be seen that for a spot size of 32 micron best sensitivity is achievable when fluidic gap distance is 1300 micrometer. This is in close agreement with the experimental result reported in [12]. For validating design data pertaining to 5,14 and 23 micrometer spot sizes, further experimental investigations are required.

However design data pertaining to optical power drop of only 34.01% (Transmittance of 65.99%) is not in agreement with earlier experimental result [12] wherein transmittance is of only 1% (when fluidic gap is 1000 micrometer) has been reported. This large difference between theoretical and actual experimental result can be explained with the help of Fig 5. From Fig. 5, it can be seen that transmittance loss is more when higher order modes are present. Decay of light is less when light propagates with lower order modes. In order to reduce the optical power loss, propagating light has to be restricted to lesser number of modes. This is achievable by reducing the refractive index contrast between the core and cladding. In our design the variation of refractive indices is from 1.5 to 1.55.

Organic light emitting diode (OLED) is one of the major element in fabricating various components required for monolithically integrated optofluidic sensor. We have fabricated an OLED and the optical power output from this light source was measured as a function of applied voltage and is shown in Fig. 10. It will be seen from Fig. 10 that optical power output up to 230 microwatts is obtainable. In this context it may be stated that peak emission from OLED is 530 nanometers and very well fits in our waveguide design. The actual photograph of glowing OLED is shown in Fig. 11. Our next step is to couple the OLED output to waveguides. Complete validation of our design data would then become feasible.

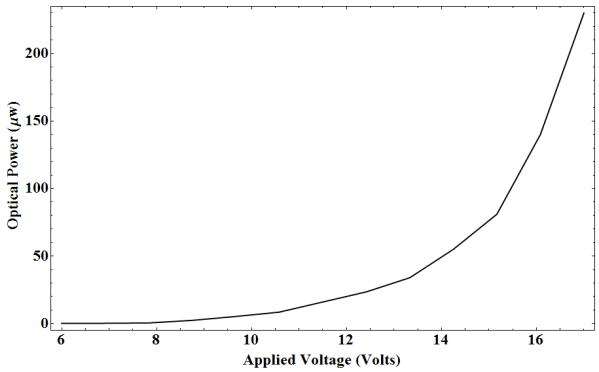

Fig 10. Plot of Optical power output verses Applied voltage.

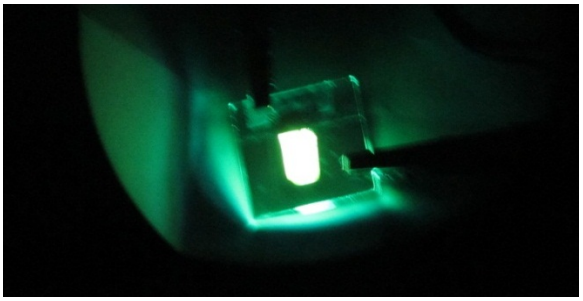

Fig 11. Photograph of the fabricated OLED emitting light at an applied voltage of 16 Volts.

VI. CONCLUSION

In this paper we have shown how the light propagates and decays in the fluidic gap. We have seen that the mode mismatch caused due to the fluidic gap can be utilized to achieve maximum sensitivity by appropriate design of fluidic channel width. We have also shown the design of integrated optical waveguide for optofluidic lab-on-a-chip application.

REFERENCES

[1] Psaltis D, Quake SR, and Yang CH "Developing optofluidic technology through fusion of microfluidics and optics," *Nature* Vol 442, pp 381-386, 27 July 2006.

[2] A.K. Sheridan, George Stewart, H, Ur-Reyman, Navin Suyal, and Deepak Uttamchandani, "In-Plane Integration of Polymer Microfluidic Channels With Optical Waveguides- A Preliminary Investigation" *IEEE Sensors Journal.,* Vol.9, No.12, pp. 1627-1632, December 2009.

[3] Cao Gua-Hua, Qin Da-Shan, Guan Min and Li Jin-Min , "Organic Light Emitting Diodes with an Organic Acceptor/ Donnor Interface Involved in Hole Injection", *Chin.Phys.Lett*., 24 No 5, 2007.

[4] Vijay Srinivasan, Vamsee K.Pamula and Richard B.Fair "Droplet Based microfluidic lab-on-a-chip for glucose detection." *Analytica Chimica Acta* 507, pp. 145-150, 2004.

[5] Andrea Pais, Ansuman Banerjee, David Klotzkin and Ian Paautsky, "High-sensitivity, disposable lab on a chip with thin-film organic electronics for fluorescence detection", *LabChip.,* 8**,** pp. 794 , 2008.

[6] S.Iraj Najafi, Paul G.Suchoski JR and Ramu V.Ramaswamy, " Silver Film-Diffused Glass Waveguides: Diffusion Process and Optical Properties" *IEEE Journal of Quantum Electronics.,* Vol. QE-22, NO.12, December 1986.

[7] Abelhak Belkhir " Detailed Study of Silver Metallic film diffusion in a soda lime glass substrate for optical waveguide fabrication" *Applied Optics.,* Vol41, No15, pp 2888-2893, May 2002.

[8] William C. Borland, David E.Zelmon, Carl L.Rades, Joseph T. Boyd, and Howard E. Jackson "Properties of four layer planar optical waveguides near cutoff", *IEEE Journal of Quantum Electronics,* Vol QE-23, No.7, July 1987

[9] Theodor Tamir, *Guided-Wave Optoelectronis*, Springer-Verlag., April 1990, pp 43-74.

[10] Clifford Pollack, *Fundamentals of Optoelectronics.*, Irwin 1995, pp 243-257.

[11] Katsunari Okamoto, *Fundamentals of Optical Waveguide.*, Second Edition, Academic Press 2006, pp. 40-44.

[12] Klaus B. Mogensen, Jamil El-Ali, Anders Wolff, and Jorg P. Kutter, "Integration of polymer waveguides for optical detectionin microfabricated chemical analysis systems" *Applied Optics*, Vol 42, No 2, pp4072-4079, 1 July 2003.